where

$$Q^{e,h} = \gamma_2\{-Y_2^{TM,TE^2}\sinh\gamma_2(t-y)\cosh\gamma_2 t - Y_1^{TM,TE^2}\cosh\gamma_2(t-y)\sinh\gamma_2 t - Y_2^{TM,TE}Y_1^{TM,TE}\cosh\gamma_2(2t-y)\}/\sinh^2\gamma_2(t-y)/v^2$$

and

$$v = \sinh\gamma_2 y\left[Y_2^{TM,TE} + Y_1^{TM,TE}\coth\gamma_2(t-y)\right] + \cosh\gamma_2 y\left[Y_1^{TM,TE} + Y_2^{TM,TE}\coth\gamma_2(t-y)\right]$$

In the electrostatic case, we can take the limit $k_0 \to 0$; and hence Eq. (8) reads

$$\tilde{\phi} = \frac{\sinh\Gamma(t-y) + \epsilon_r\cosh\Gamma(t-y)}{\epsilon_r\cosh\Gamma t + \sinh\Gamma t}\,\frac{4\pi a\,\Delta J_1(a\Gamma)\,m_\phi}{\Gamma} \tag{11}$$

where $\Gamma = \sqrt{\alpha^2 + \beta^2}$.

SUMMARY

The electric field and electric potential due to a thin, magnetic-current loop radiating just above the ground plane of a grounded dielectric slab are derived. The electric potential in the electrostatic case is then obtained by setting $k_0 = 0$. These expressions are useful for the characterization of the microstrip, via, and via hole discontinuities appearing in computer circuit-board packaging.

REFERENCES

1. A. J. Blodgett, Jr., "Microelectronic Packaging," *Scientific American*, July 1983, pp. 86–97.
2. T. Wang, R. F. Harrington, and J. R. Mautz, "Quasi-Static Analysis of a Microstrip Via through a Hole in a Ground Plane," *IEEE Trans. Microwave Theory Tech.*, Vol. MTT-36, June 1988, pp. 1008–1013.
3. C. M. Butler and R. Umashankar, "Electromagnetic Penetration through an Aperture in a Finite, Planar Screen Separating Two Half Spaces of Different Electromagnetic Properties," *Radio Science*, Vol. 11, July 1976, pp. 611–619.
4. T. Itoh, "Spectral Domain Immitance Approach for Dispersion Characteristics of Generalized Printed Transmission Lines," *IEEE Trans. Microwave Theory Tech.*, Vol. MTT-28, July 1980, pp. 733–736.
5. C. H. Chan, K. T. Ng, and A. B. Kouki, "A Mixed Spectral Domain Approach for Dispersion Analysis of Suspended Planar Transmission Lines with Pedestals," *IEEE Trans. Microwave Theory Tech.*, to be published.

Received 2-3-89

Microwave and Optical Technology Letters, 2/5, 157–159

CCC 0895-2477/89/$4.00

OPTICALLY EXCITED MICROWAVE RING RESONATORS IN GALLIUM ARSENIDE

Douglas S. McGregor, Chang Soo Park, Mark H. Welchold, Henry F. Taylor, and Kai Chang
Department of Electrical Engineering
Texas A & M University
College Station, Texas 77843

KEY TERMS

Ring resonator, microwave–optical interactions, gallium arsenide, microwave generation

ABSTRACT

Microstrip ring resonators with fundamental frequencies near 3.5 GHz have been fabricated in semi-insulating GaAs using an electroplating technique for conductor deposition. Test signals were coupled into the resonators by focusing modulated light into a photoconductive microstripline gap. Loaded Q-factors measured for one of the rings with optical excitation ranged from 54 at the fundamental frequency to 03 at the third harmonic.

There is increasing interest in the use of optical techniques in the characterization of high-speed GaAs integrated circuits. Pulses from modelocked lasers provide picosecond sampling

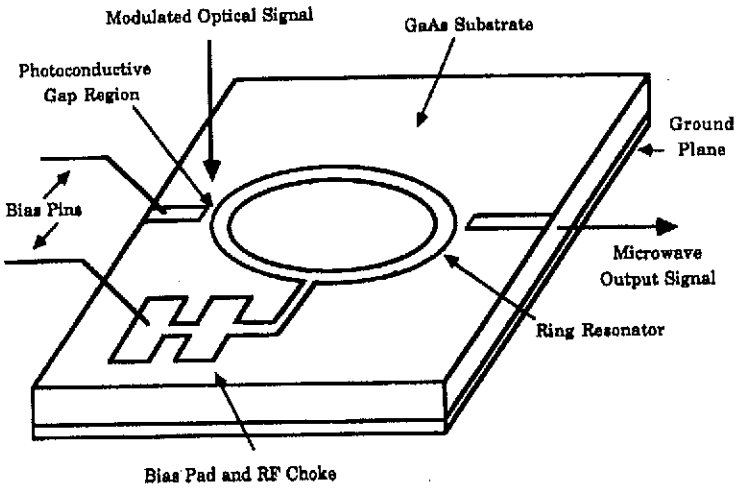

Figure 1 Configuration for ring resonator in GaAs.

windows for noninvasive probing of voltage waveforms in GaAs integrated circuits [1, 2]. The use of optically injected carriers for the generation of short electrical pulses in the measurement of microstrip transmission line response has also been reported [3, 4].

Previous work on optical characterization of electronic and microwave circuits has concentrated upon the use of short optical pulses for time-domain response measurements. This paper describes the application of optical signal injection for frequency-domain characterization of microwave circuits. Optical excitation provides a means of introducing waveforms into the circuit while avoiding transmission line effects and interconnections associated with conventional microwave probes. The microstrip ring resonator [5, 6] was chosen for study as a simple test circuit in which the frequency-domain response to optical excitation can readily be measured. The fabrication of the resonators on GaAs substrates and their microwave and optical characterization are described.

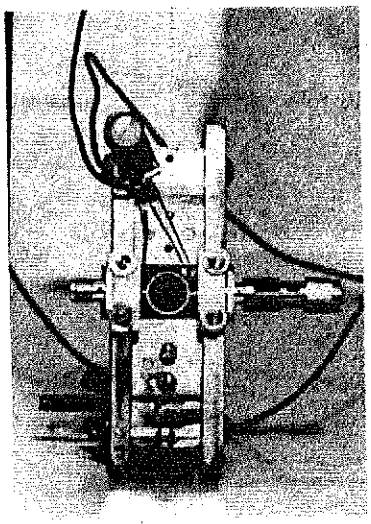

Figure 2 Ring resonator in microwave test fixture.

The resonator circuit configuration is illustrated in Figure 1. The undoped semi-insulating GaAs substrates had resistivities in the 10^7 Ω-cm range. The substrate thickness of 0.015 inch was chosen to maximize the resonator Q-factor near 10 GHz [7]. The microstrip lines were 274 μm wide, the ring diameter to the center of the lines was 4.72 mm, and the gaps separating the feeder lines from the rings were 3 μm across. A pad attached to one side of the ring through an inductive ac block was used to apply a dc bias across one of the gaps for the optical measurements.

A plate-through process was used to fabricate the thick Au electrodes for the resonators. After deposition of a groundplane electrode on the reverse side of the substrate, 750 Å of Au–Ge followed by 105 Å of Ni were evaporated onto the front of the wafer. The desired electrode pattern was then defined photolithographically in positive resist, which served as a mask during the plating process. After a hard bake at 135°C, 3.5 μm of Au was plated through the mask. The photoresist and the thin Au–Ge–Ni layer in the unplated region were removed, and the substrate was then annealed for 2 min at 450°C with a resistive strip heater to promote diffusion of the Au–Ge underlayer into the GaAs. This produced ohmic contact between Au electrodes and the substrate.

Microwave measurements were made using a test fixture designed for gentle handling and easy interchangeability of the brittle substrates [8]. A photograph of one of the resonators in the test fixture is shown in Figure 2. The S_{21} characteristic for this device measured with a Hewlett-Packard 8510A network analyzer is shown in Figure 3. The resonator peaks are at 3.475, 6.885, and 10.295 GHz. Additional structure can be attributed to reflections from the rf choke and bias pad.

Optical excitation was accomplished by focusing the light from a current-modulated 0.843-μm semiconductor laser supplied by Ortel into one of the gaps between a feed line and the ring. Threshold current for the laser was 20 mA and it was operated at a dc bias level of 25 mA. The laser package

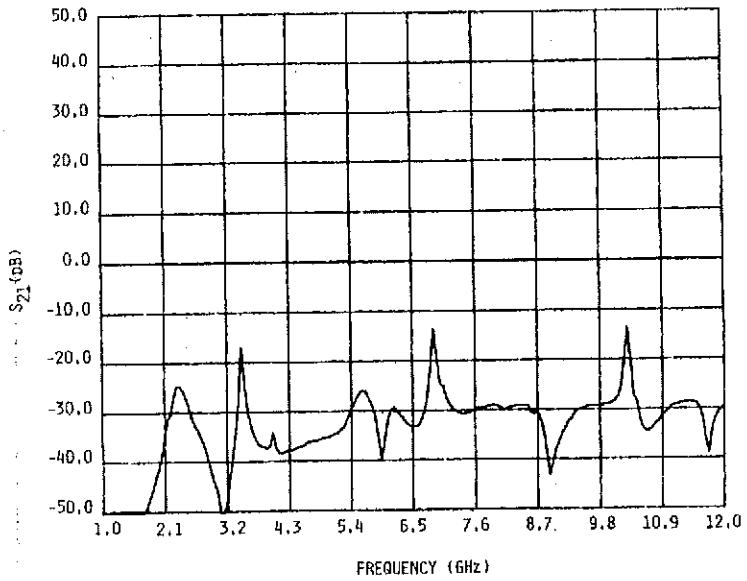

Figure 3 S_{21} spectrum for ring resonator.

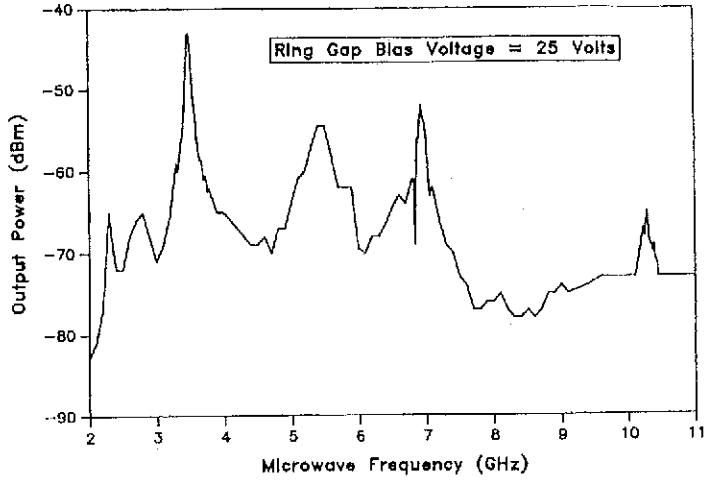

Figure 4 Microwave output spectrum from ring resonator with optical excitation for a gap bias of 25 V.

contained a series resistor for impedance matching to a 50-Ω transmission line. A microwave power of about −15 dBm was supplied to the laser through a bias tee by a Hewlett-Packard 8340A synthesized sweeper. The microwave output power spectrum from the ring as measured with a Hewlett-Packard 8565A spectrum analyzer is plotted in Figure 4 for a 25-V dc bias applied across the resonator gap. Output peaks corresponding to the first three resonances appeared 3.48, 6.89, and 10.30 GHz, close to the values observed in the microwave measurements. The loaded Q-values at these frequencies were 54, 75, and 103, respectively. This increase in Q with frequency is expected because the substrate thickness was chosen to minimize the microstrip loss near 10 GHz. Corresponding microwave power levels at the first three resonances were −43, −52, and −65 dBm. The 22-dB decrease in microwave response from the fundamental to the third harmonic compares with an 18-dB reduction in microwave from the laser over the frequency range from 3.5–10.3 GHz, as measured with a photodetector with a 3-dB bandwidth of 8 GHz. The microwave output power was an increasing function of the gap bias voltage, as illustrated in Figure 5.

In conclusion, ring resonators in GaAs have been characterized with microwave and optical excitation. The results demonstrate the use of optical signal injection for frequency-domain characterization of a simple monolithic microwave circuit element. Optical injection eliminates transmission line effects which are present when microwave probes are used.

ACKNOWLEDGMENTS

The authors would like to thank Fuchen Wang for helping with the ring design and Michael Skrehot for helpful discussions. This work was supported by the Office of Naval Research.

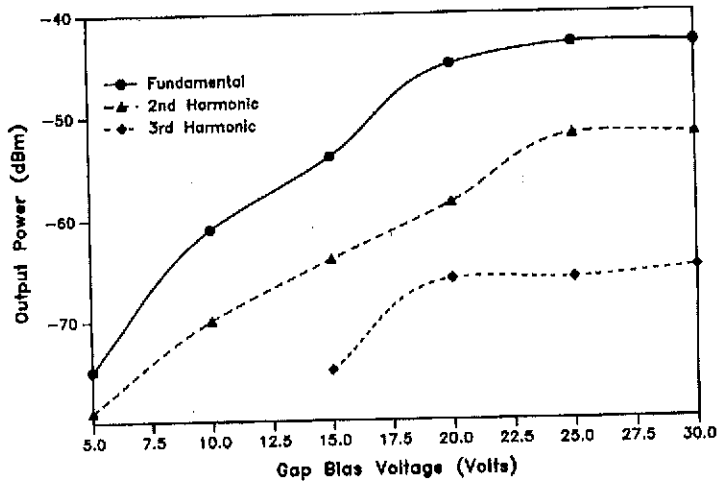

Figure 5 Dependence of microwave power from the ring under optical excitation on the dc bias voltage applied across the microstripline gap.

REFERENCES

1. J. A. Valdmanis and G. Morou, "Subpicosecond Electroopic Sampling, Principles and Application," *IEEE J. Quantum Electron.*, Vol. QE-22, January 1986, pp. 69–78.
2. K. J. Weingarten, M. J. Rodwell, and D. M. Bloom, "Picosecond Sampling of GaAs Integrated Circuits," *IEEE J. Quantum Electron.*, Vol. QE-24, February 1988, pp. 198–220.
3. D. G. Grischkowsky, M. Ketchen, C. C. Chi, I. N. Duling, N. J. Halas, J. M. Halbout, and P. G. May, "Capacitance Free Generation and Detection of Subpicosecond Electrical Pulses on Coplanar Transmission Lines," *IEEE J. Quantum Electron.*, Vol. QE-24, February 1988, pp. 221–239.
4. J. A. Valdmanis, "One THz Bandwidth Prober for High-Speed Devices and Integrated Circuits," *Electron. Lett.*, Vol. 23, November 1987, pp. 1308–1310.
5. H. J. Finlay, R. H. Jansen, J. A. Jenkins, and I. G. Eddison, "Accurate Characterization and Modeling of Transmission Lines for GaAs MMIC's," *IEEE Trans. Microwave Theory Tech.*, Vol. MTT-36, June 1988, pp. 961–966.
6. R. E. Neidert and S. C. Binari, "mm-Wave Passive Components for Monolithic Circuits," *Microwave J.*, April 1984, pp. 103–116.
7. K. Chang, F. Hsu, J. Berenz, and K. Nakano, "Find Optimum Substrate Thickness for Millimeter GaAs MMICs," *Microwaves and RF*, September 1984, pp. 123–128.
8. D. S. McGregor and M. H. Weichold, "An Improved Microwave Test Fixture for Brittle Substrate Materials," *Rev. Sci. Instru.*, March 1989, to be published.

Received 2-13-89

Microwave and Optical Technology Letters, 2/5, 159–162

CCC 0895-2477/89/$4.00

IFM RECEIVER WITH CAPABILITY OF DETECTING SIMULTANEOUS SIGNALS

James B. Y. Tsui
Wright-Patterson Air Force Base
Ohio 45433

KEY TERMS

Microwave receiver, signal processing, electronic warfare

ABSTRACT

A method for detecting many simultaneous signals in an IFM receiver is described. The method uses correlation lags to calculate the frequencies of the input signals. Practical considerations and performance are discussed.

1. INTRODUCTION

An instantaneous frequency measurement (IFM) receiver uses phase correlators to obtain the correlations of different lags of the input signal to measure its frequency [1–3]. Conventional IFM receivers have relatively wide input bandwidth—sometimes extending over one octave. The receiver can measure frequency accurately on short pulses. One major deficiency of an IFM receiver is that the receiver cannot measure simultaneous signals. Worst yet, under simultaneous signal conditions, the receiver may generate an erroneous frequency report. The erroneous frequency report which cannot be recognized will cause tremendous problems to the digital processor following the receiver. Even the detection of the existence of simultaneous signals is useful information to the digital signal processor. This deficiency of the IFM limits its applications in electronic warfare (EW) receiving systems.

This paper presents a theoretical approach which takes the outputs of the phase correlators and performs the proper mathematical operations to obtain the frequency (or frequencies) of the input signal. Theoretically, this method can be used to solve many simultaneous signals. It has closed-form solutions for up to four frequencies by finding the roots of a fourth-order polynomial. Beyond four frequencies numerical solutions can be used. In the next section, an IFM receiver operating under simultaneous signal conditions will be briefly discussed. In Section 3, the basic idea of measuring simultaneous signals will be discussed. In Section 4, different choices of correlation lags are employed to save hardware. In Section 5, the performance of an IFM receiver will be discussed.

2. CORRELATOR OUTPUTS AND SIMULTANEOUS SIGNAL CONDITIONS

The phase correlator in an IFM receiver is made of power divider, delay line, 90° and 180° hybrids, video detectors, differential amplifiers, and low-pass video filters [4]. The outputs of a correlator with delay time τ and input signal $A\sin(\omega t)$ where A is the amplitude and ω is the angular frequency can be written as

$$\begin{aligned} R_r(\tau) &= P\cos(\omega\tau) \\ R_i(\tau) &= P\sin(\omega\tau) \end{aligned} \tag{1}$$

where $P = A^2/2$ represents the power of the input signal. The above equations can be written in complex form as

$$R(\tau) = R_r(\tau) + jR_i(\tau) = P\exp(j\omega\tau) \tag{2}$$

where $j = \sqrt{-1}$ represents the imaginary operator.

The input frequency can be found as

$$\omega = (1/\tau)\tan^{-1}(R_i/R_r) \tag{3}$$

There are two simultaneous signal conditions: leading-edge time-coincident and noncoincident [5]. Here the discussion will be concentrated on the leading-edge time-coincident case. In order to keep the discussion simple, let us first consider only two signals and also assume that the frequency separation is far apart such that the difference frequency will be filtered out by the low-pass video filter in the correlator. Under these conditions, the outputs from the correlator are

$$\begin{aligned} R_r(\tau) &= P_1\cos(\omega_1\tau) + P_2\cos(\omega_2\tau) \\ R_i(\tau) &= P_1\sin(\omega_1\tau) + P_2\sin(\omega_2\tau) \end{aligned} \tag{4}$$

where P_1 and P_2 are the power of the signal with frequency ω_1 and ω_2. If one still uses Eq. (2) to find the input frequency, the result will be erroneous. If $P_1 = P_2 = P$, the result is

$$\begin{aligned} \omega &= \frac{1}{\tau}\tan^{-1}\left[\frac{\sin(\omega_1\tau) + \sin(\omega_2)}{\cos(\omega_1\tau) + \cos(\omega_2)}\right] \\ &= \frac{1}{\tau}\tan^{-1}\left[\tan\left(\frac{\omega_1 + \omega_2}{2}\tau\right)\right] \\ &= \frac{\omega_1 + \omega_2}{2} \end{aligned} \tag{5}$$